JOURNAL OF CATALYSIS 82, 299–312 (1983)

X-Ray Absorption Edge and Extended X-Ray Absorption Fine Structure Studies of Pt/TiO_2 Catalysts

D. R. SHORT,[1] A. N. MANSOUR,* J. W. COOK, JR.,*
D. E. SAYERS,* AND J. R. KATZER[2]

*Center for Catalytic Science and Technology, Department of Chemical Engineering, University of Delaware, Newark, Delaware 19711; and *Department of Physics, North Carolina State University, Raleigh, North Carolina 27650*

Received August 26, 1981; revised March 3, 1983

X-Ray absorption edge and extended x-ray absorption fine structure (EXAFS) spectroscopy was used to study Pt/TiO_2 prepared by two different techniques. Edge studies show that the observable electronic structure of very small particles of reduced Pt/TiO_2 are independent of preparation technique. After H_2 reduction at 473°K, Pt/TiO_2 has about 10% fewer unfilled (vacant) *d* states (0.03 fewer *d* state vacancies) per Pt atom than Pt/SiO_2, prepared and reduced the same way, and has about 15% more unfilled *d* states (0.04 more *d* state vacancies) per Pt atom than bulk Pt. Reduction of Pt/TiO_2 in H_2 at 698°K results in less than a 4% reduction in the number of unfilled *d* states per Pt atom (less than 0.015 hole reduction per Pt atom) as compared to the 473°K reduction, indicating a very small amount of electron transfer to the Pt induced by the high-temperature H_2 reduction of Pt/TiO_2. It was concluded that the reported effect of high-temperature reduction of Pt/TiO_2 on CO and H_2 chemisorption is not due to a substantial change in the extent of electron transfer from the support but is due to more subtle and specific electronic changes.

INTRODUCTION

Although the primary motivation for the high dispersion of a metal on a support such as silica or alumina is often economic, i.e., better utilization of the metal, the presence of the support and the degree of dispersion can greatly influence the observed catalytic properties (*1, 2*). Some of these effects can be due to interactions with the support. The details of the interaction of a metal with its support and the effect of the interaction on the catalytic activity of the metal are not understood. Recent studies of H_2 and CO chemisorption on noble metals supported on TiO_2 or on oxides of certain Group VB metals have yielded interesting results in this regard (*3, 4*). A drastic reduction in the chemisorption of H_2 or CO on Pt/TiO_2 after reduction at high temperatures (673–773°K) has been observed (*3*). This decrease was not due to an increase in metal particle size or a loss in metal surface area (*5, 6*) and was shown to be reversible by reoxidation (*6*). This led to the hypothesis of strong metal-support interactions (SMSI) (*3*) and to suggestions of metal–metal bondings or the formation of intermetallic compounds with the support. Scattered-wave X-α molecular orbital calculations based upon two different models of Pt on TiO_2 have indicated the possibility of the donation of electron-charge density from Ti^{3+} surface sites to Pt (*7*). These possibilities have been supported by single-crystal Auger and photoemission studies of platinum on $SrTiO_3$ (*8, 9*) and by XPS studies of Pt/TiO_2 after reduction at high temperature (773°K) (*10*).

Recently it has been suggested (*11*) that the SMSI has both a structural and an elec-

[1] To whom all correspondence should be addressed. Current address: Engineering Technology Laboratory, Experimental Station, E. I. du Pont de Nemours and Co., Inc., Wilmington, Delaware 19898.

[2] Current address: Central Research Department, Mobil Research and Development Corporation, Princeton, New Jersey 08540.

0021-9517/83 $3.00

tronic component. Structurally, the change in Pt crystallite morphology observed by electron microscopy upon high-temperature reduction of Pt/TiO_2 and the accompanying change in the oxidation state of significant numbers of surface Ti ions has been interpreted (*11*) as evidence for the formation of strong bonds between the "pill box"-shaped supported crystallites and the reduced surface Ti^{3+}. The importance of electronic interactions has been recognized (*11*), and the strong bonding interaction has been interpreted as predominantly due to strong ionic attractions between atoms of the supported metal and surface Ti^{3+}, which result through charge transfer from the reduced cation to the adjacent metal atom and the acquisition of substantial negative charge by the metal crystallite. The decrease in H_2 and CO chemisorption in the SMSI state has been suggested to be due to an accompanying increase in the Pt–Pt distance, which weakens the interaction between metal atoms and gas molecules, or to be due to the strongly ionic character of the hypothesized bond between surface Ti^{3+} and metal atoms which may interfere with electron transfer from the metal atoms to gas molecules. The latter explanation, at least, would most likely require an extensive degree of metal-cation bonding to explain the drastic decrease in chemisorption behavior observed.

The structural and electronic changes, including the potential of special Pt–Ti interactions, which are associated with higher temperature reduction need to be more fully investigated. The effects of metal-support interactions should be most significant in supported metal systems characterized by high degrees of dispersion, but these systems are not open to investigation by many experimental techniques. X-Ray absorption edge and Extended X-ray Absorption Fine Structure spectroscopy (EXAFS) can provide information about electronic and atomic structure in the immediate vicinity of the atom of the absorbing element without the stringent requirement of long-range structural order. Thus, x-ray edge and EXAFS spectroscopy can provide unique structural information on highly dispersed supported metals (*12–17*).

The structure of the L_{II} and L_{III} absorption edges are the result of electronic transitions from the $2p_{1/2}$ and $2p_{3/2}$ core levels, respectively, to empty $6s$ and $5d$ states (*18, 20*). A correlation between the energy dependent Pt L_{III} edge absorption coefficient, corrected for support absorption, and corresponding data for bulk Pt metal has been interpreted in terms of changes in the electron density in bonds at or above the Fermi level upon adsorption of various gases on small supported crystallites of Pt (*21, 22*). Correlations between the area under only the L_{III} absorption edge and d band vacancies have been used previously to investigate the electronic characteristics of supported materials (*14, 23, 24*). However, such correlations neglect to account for the L_{II} edge absorption, which involves $d_{3/2}$ final states. Recent work by Mansour *et al.* (*25*) has shown that the area under the absorption spectrum in the near edge region of both the L_{II} and L_{III} edges can be systematically and quantitatively related to the number of unoccupied d states associated with the absorbing atoms. Application of this method to study the effects of different reduction temperatures on other supported Pt catalysts have shown that changes in the unoccupied d states of less than 0.1 electron/atom can be detected (*26*).

We present here the results of x-ray absorption edge and EXAFS studies of two samples of highly dispersed Pt/TiO_2 prepared by different methods and reduced at several temperatures in flowing H_2 immediately preceding the x-ray absorption measurements. The objectives of the study were to determine the direction and extent of any charge transfer between platinum and the support, and to characterize any physicochemical or structural changes which occur in the vicinity of the Pt atoms as a function of increasing reduction temperature.

EXPERIMENTAL

The TiO_2 was prepared from titanium isopropoxide (TYZOR, obtained from Du Pont) by hydrolyzing with water, washing the precipitate, drying for 24 h at 393°K, and calcining at 673°K in flowing O_2 for 2 h. The resultant material was predominantly anatase and has a BET surface area of about 120 m^2/g. One sample of Pt/TiO_2 was prepared by "impregnation" using the "incipient wetness" method. A known mass of TiO_2 was contacted with a measured volume of solution sufficient to fill the TiO_2 pore structure and containing a known amount of Pt as $(NH_3)_4Pt(NO_3)_2$ (Johnson Matthey, Inc.). The sample was allowed to stand for 10 days to allow equilibration of Pt throughout each particle before drying in air at 393°K. A second Pt/TiO_2 sample was prepared by "ion exchange." The TiO_2 was slurried with a solution of $(NH_3)_4Pt(NO_3)_2$ and allowed to equilibrate for 24 h. It was then filtered and washed with deionized water and dried in air at 393°K.

Analysis by atomic absorption spectroscopy indicated that the "ion-exchanged" Pt/TiO_2 contained 1.7 wt% Pt and that the "impregnated" Pt/TiO_2 contained 3.1 wt% Pt. Transmission electron microscopy studies showed that the 1.7 wt% Pt/TiO_2 was very well dispersed, having all platinum crystallites less than 15 Å. The TEM studies of the 3.1 wt% Pt/TiO_2 indicated very small Pt particles, also less than 15 Å in size, with apparently some larger Pt particles. Hydrogen chemisorption on both samples after 473°K reduction in flowing dry H_2 gave 1.0 H atom adsorbed per Pt for the ion-exchanged Pt/TiO_2 and 0.86 for the impregnated Pt/TiO_2. Hydrogen chemisorption of these samples after reduction at 723°K indicated negligible adsorption of H_2, in agreement with published results (*3*). FTIR studies of chemisorbed CO as a function of CO pressure suggested that the ion-exchanged Pt/TiO_2 was very highly dispersed as indicated by the absence of any effect of CO pressure on CO band position. The band position of CO adsorbed on the impregnated Pt/TiO_2 increased by 30 cm^{-1} with increasing CO pressure, suggesting some larger, more metallic-like Pt surfaces, i.e., larger Pt particles.

Portions of both samples were ground to powder and pressed into separate wafers for x-ray absorption spectroscopy. The wafer thickness was chosen to yield an incident intensity to transmitted intensity ratio of 3 to 5. All samples were mounted in cells, described elsewhere (*17*), which were heated slowly (~3°K/min) to 623°K and held there for 1 h in flowing O_2. Hydrogen reduction at the temperatures of interest was also carried out in the absorption cell. Each reduction involved a slow rise to the final temperature (3°K/min), maintenance of this temperature for 1 to 2 h, followed by cooling to room temperature, all under flowing H_2. The cells were checked for high-vacuum integrity prior to use.

The x-ray absorption experiments were performed on x-ray beam line I-5 (*27*) at the Stanford Synchrotron Radiation Laboratory (SSRL), with ring energies of approximately 3.0 GeV and ring currents between 50 and 80 mA. The L_{III} and L_{II} absorption edges were taken on each sample at liquid nitrogen temperature and under slightly less than 1 atm pressure of static H_2. The corresponding absorption edges of a 1-μm-thick platinum foil were employed as references for fixing the energy scale and as a standard in subsequent calculations relating to absorption edge and EXAFS analysis. Each absorption spectrum required about 30 min counting time.

Analysis of data from the near edge region of the absorption edges followed the technique of Mansour *et al.* (*25*). Analysis of the EXAFS data first involved fitting a smooth, cubic spline function to the data above the edge and substracting this background from the data, leaving the oscillatory EXAFS function $\chi(k)$ versus k, the photoelectron wave vector. This was followed by Fourier transformation of the k^3 weighted fine structure over a k range of 2.2

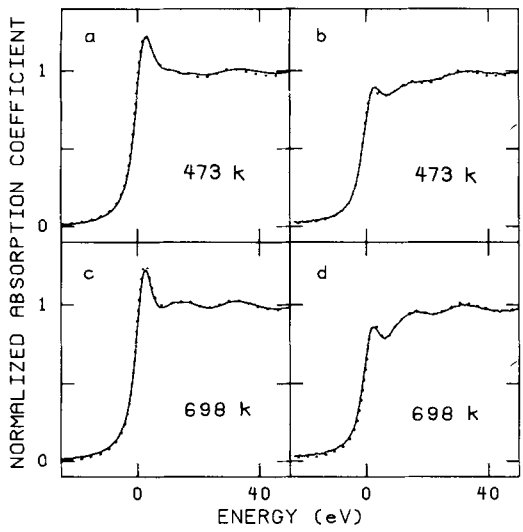

FIG. 1. Comparison of the L_{III} (a and c) and L_{II} (b and d) absorption edges of 1.7 wt% Pt/TiO_2 (—) and 3.1 wt% Pt/TiO_2 (---) after H_2 reduction at the indicated temperature.

to 11.0 $Å^{-1}$ for the 1.7 wt% samples and 2.2 to 13.7 for the 3.1 wt% samples to obtain a radial structure function. The portion of the radial structure function corresponding to the first main peak was then selected by filtering out those frequencies not belonging to the first shell and transforming back to *k*-space. These back-transformed data were then analyzed for the distance, the coordination number, and the relative thermal disorder of the first shell, both by using nonlinear least squares fitting with experimental parameters for Pt–Pt and Pt–O bands from Pt metal and oxide reference data and theoretical Ti parameters (*28*) to specify the kinds of atoms in the first coordination shell, and by using a direct ratio of the experimental data with Pt foil as described previously (*29*).

RESULTS

X-Ray Absorption Edge Studies

The normalized L_{II} and L_{III} edge structure of both the impregnated and ion-exchanged Pt/TiO_2 samples after H_2 reduction at the indicated temperature are compared in Fig. 1. The zero in energy for each curve is taken to be the inflection point on the rapidly rising absorption edge. Figure 1 shows that for a particular absorption edge and a given H_2 reduction temperature, the curves for the 3.1 and the 1.7 wt% Pt/TiO_2 samples coincide, with no significant deviation over most of the edge region. For the samples reduced in H_2 at 473°K, very small differences appear between samples beyond about 20 eV above the absorption edge. There is a difference in the magnitude of the EXAFS of these two samples, and the differences observed in this near-edge region are probably due to differences in the EXAFS magnitude although it is not possible to state unequivocally where the edge structure ends and the extended fine structure begins. Therefore, in the following discussion, we define the near-edge region to include that region of the spectrum from −10 to +20 eV about the edge.

Although the edge structures are independent of preparation procedure and H_2 reduction temperature (Fig. 1), there are significant differences in both the L_{III} and L_{II} near-edge structures of the small crystallites of platinum supported on TiO_2 as compared with a 1-μm thick Pt foil (Fig. 2).

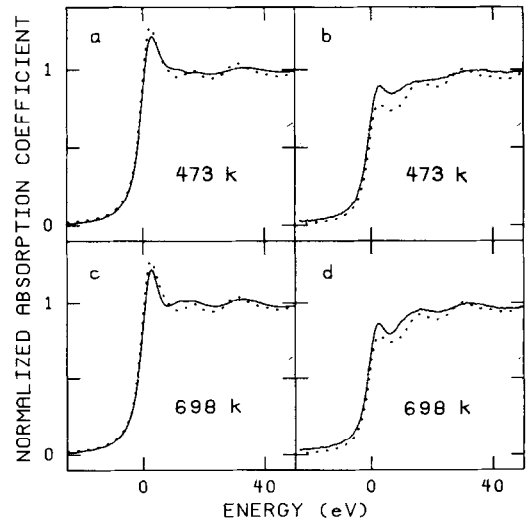

FIG. 2. Comparison of the L_{III} (a and c) and L_{II} (b and d) absorption edge of 1.7 wt% Pt/TiO_2 (—) after H_2 reduction at the indicated temperature with that of a 1-μm Pt foil (---).

For the L_{III} edge of Pt/TiO_2, Figs. 2a and c show that the edge or white-line peak is reduced relative to that of the foil edge at both H_2 reduction temperatures. The 473°K H_2 reduction produces a white-line peak which is slightly broader at its base than that of the foil, while the 698°K reduction results in a white line which is narrower than that of the foil (Fig. 2c). The L_{II} edge of both Pt/TiO_2 samples has a higher peak at the edge than the foil (Figs. 2b and d), and this increased absorption persists over the entire near-edge region. We have also measured the 3.1 wt% Pt/TiO_2 after H_2 reduction at 573°K in H_2 and find that the edge structures are intermediate between those for the 473 and 698°K reduction for both absorption edges.

Figure 2 shows that highly dispersed Pt/TiO_2 is characterized by electronic transitions above the L_{II} and L_{III} absorption edges which have different probabilities from those of bulk Pt. The area under the Pt L_{III} absorption edge is significantly smaller for the Pt/TiO_2 samples reduced in H_2 at 473°K and at 698°K as compared with the corresponding area for bulk Pt. On the other hand, the area under the Pt L_{II} absorption edge for the Pt/TiO_2 after H_2 reduction at either temperature is significantly larger than the area under the L_{II} edge for bulk Pt. Thus, the net change in the combined L_{III} and L_{II} edge areas of the Pt/TiO_2 in relation to the combined edge areas of bulk Pt amounts to a slight increase when calculated by the method of Mansour *et al.* (*25*); this indicates a small increase in the number of *d*-band electron vacancies (unfilled *d* states) for these samples after either H_2 reduction temperature relative to bulk Pt. In other studies we have shown that small crystallites of Pt supported on either SiO_2 or Al_2O_3 have the same L_{II} and L_{III} absorption edge areas after H_2 reduction at 723°K, which yields their most reduced state (*26*). In both cases, the supported Pt exhibits a similar deficit in *d*-band electron density relative to bulk Pt. It is appropriate, therefore, to compare the near-edge structure of the Pt/TiO_2 catalysts with the edge structure of small Pt crystallites on one of these supports.

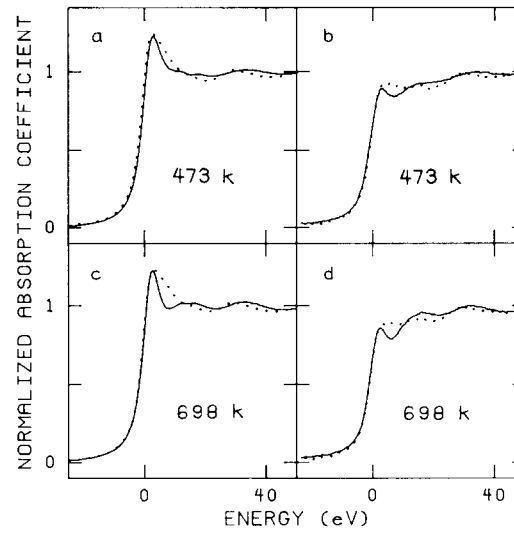

FIG. 3. Comparison of the L_{III} (a and c) and L_{II} (b and d) absorption edges of 1.7 wt% Pt/TiO_2 (—) reduced in flowing H_2 at 473 and 698°K with those of 0.7 wt% Pt/SiO_2 (---) reduced at 473 and 723°K.

Since the interaction of Pt atoms with the surface of SiO_2 is expected to be lower than that for most other supports, a highly dispersed sample of Pt/SiO_2 which we have characterized elsewhere (*26*) was chosen for comparison with the Pt/TiO_2 samples. The L_{II} and L_{III} absorption edges of the 0.7 wt% Pt/SiO_2 (having <15 Å Pt crystallites) were independent of H_2 reduction temperature between 473 and 723°K (*26*). Comparisons between normalized absorption edges of the 1.7 wt% Pt/TiO_2 and 0.7 wt% Pt/SiO_2 are shown in Fig. 3. The L_{III} orL_{II} edge peak height is the same for the Pt/TiO_2 and the Pt/SiO_2, although the areas of the L_{III} and L_{II} edges are significantly smaller for the Pt/TiO_2 than for the Pt/SiO_2. The L_{III} edges of the Pt/TiO_2 samples are narrower on the high-energy side of the white line than for Pt/SiO_2 at both H_2 reduction temperatures. The Pt/TiO_2 edge narrows significantly with increasing reduction temperature. The L_{II} edges of Pt/TiO_2 immediately following the edge peak are decreased relative to the L_{II}

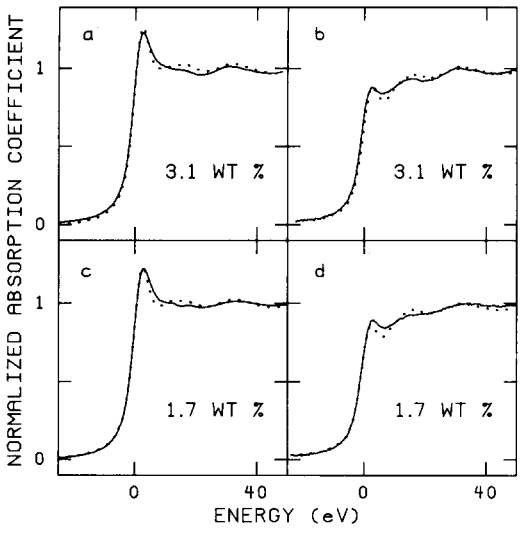

FIG. 4. Comparison of L_{III} (a and c) and L_{II} (b and d) absorption edges of indicated Pt/TiO_2 samples reduced in flowing H_2 at 473°K (—) and at 698°K (---).

near-edge region of Pt/SiO_2 and again a narrowing of the peak at the L_{II} edge of Pt/TiO_2 is observed with increasing reduction temperature. However, these results, when compared with the observations of Figs. 1 and 2, indicate that the differences in unoccupied *d*-band character between the Pt/TiO_2 and Pt/SiO_2 are significantly less than the differences between these catalysts and bulk Pt, and that the catalysts have more unoccupied *d* states than bulk Pt in each case. The small differences seen in Fig. 3 between Pt/TiO_2 and Pt/SiO_2 indicate a somewhat smaller number of unoccupied *d* states for the Pt/TiO_2 system in comparison to the Pt/SiO_2 system.

Figure 4 compares the L_{II} and L_{III} edges of Pt/TiO_2 as a function of H_2 reduction temperature. The width of the L_{III} absorption edges decreases with increasing H_2 reduction temperature, with no significant changes in peak height or position (Figs. 4a and c). This leads to an overall decrease in L_{III} edge area with increasing H_2 reduction temperature, which is mitigated somewhat, but not completely, in the region between 10 and 20 eV beyond the L_{III} edge. The height of the L_{II} edge peaks for both Pt/TiO_2 samples is the same after H_2 redution at either temperature, but the areas under the absorption curve for the 698°K reduction are smaller than those for the 473°K reduction. Thus, the areas under both the Pt L_{III} and L_{II} absorption edges decrease with increasing H_2 reduction temperature; this is direct though slight evidence for an increased electron density on Pt atoms after high-temperature reduction of the Pt/TiO_2 as compared with the low-temperature reduction. The high-temperature reduction state of Pt/TiO_2 has frequently been called the SMSI state; this is the state or condition which does not absorb either H_2 or CO (*3–6*).

Table 1 summarizes the Pt L_{II} and L_{III} edge parameters of thePt/TiO_2 samples; Pt foil is used as the reference. The edge areas decrease only slightly with increasing H_2 reduction temperatures, and the L_{II} edge is about 10% larger than that of bulk Pt after 473°K reduction in H_2. The L_{III} edge positions of all Pt/TiO_2 samples are shifted to higher energy, suggestive of a positive charge on the absorbing atom. This is consistent with the suggestion from edge peak areas that the small Pt particles are positively charged due to electron transfer to the TiO_2.

Following the work of Mansour *et al.* (*25*) the fractional change in the number of *d* band vacancies (unfilled *d* states) from that of bulk Pt, f_d, can be defined as

$$f_d = \frac{\Delta(h_T)}{(h_T)_{Pt}} = \frac{(\Delta A_3 + 1.11\Delta A_2)}{(A_3 + 1.11\,A_2)_{Pt}}, \quad (1)$$

where

$\Delta(h_T) = (h_T)_{sample} - (h_T)_{Pt}$
$\Delta A_3 = (A_3)_{sample} - (A_3)_{Pt}$
$\Delta A_2 = (A_2)_{sample} = (A_2)_{Pt}$
h_T = total number of unoccupied *d* states
A_i = edge area for the *i*th edge
Pt = bulk platinum.

Table 1 gives the calculated f_d values for each of the samples; the values are all positive indicating that the highly dispersed

TABLE 1

X-Ray Absorption Edge Parameters of Pt/TiO_2

Sample	Reduction temp. (°K)	Reduction time (h)	L_{III} edge shift, (eV)	Normalized L_{III} edge area[a]	Normalized L_{II} edge area[b]	f_d[c]	Number of unfilled d states per atom[d]
3.1 wt% Pt/TiO_2	473	1	+0.9	1.00	1.10	0.15	0.34
3.1 wt% Pt/TiO_2	573	1	+1.2	1.00	1.09	0.13	0.34
3.1 wt% Pt/TiO_2	698	1	+1.2	1.00	1.08	0.10	0.33
1.7 wt% Pt/TiO_2	473	2	+1.0	0.99	1.10	0.12	0.34
1.7 wt% Pt/TiO_2	698	1	+1.1	0.99	1.09	0.10	0.33
Pt Foil	—	—	0.0	1.00	1.00	0.00	0.30
0.7 wt% Pt/SiO_2	723	2				0.23	0.37
Estimated errors			±0.5	±0.08	±0.08	±0.02	±0.006

[a] Equal to $A_{3_{sample}}/A_{3_{Pt}}$ from technique of Mansour *et al.* (*25*).
[b] Equal to $A_{2_{sample}}/A_{2_{Pt}}$ from technique of Mansour *et al.* (*25*).
[c] Calculated using Eq. (1) by technique of Mansour *et al.* (*25*).
[d] Calculated using Eq. (2) and assuming 0.30 unfilled d states per Pt atom in bulk Pt (*20, 31, 32*).

supported Pt has a larger number of unfilled d states than the bulk Pt. Expression (1) can be rearranged to give

$$h_T|_S = [1.0 + f_d](h_T)_{Pt} \qquad (2)$$

from which the number of unfilled or vacant d states for the Pt/TiO_2 can be calculated if the number of unfilled or vacant d states is known for bulk Pt. Band structure calculations suggest that there are between 0.3 and 0.4 vacant d states per Pt atom for bulk Pt (*20, 31, 32*). Assuming 0.30 unfilled d states per Pt atom for bulk Pt, the number of unfilled d states per Pt atom for the samples was calculated (Table 1).

The Pt/TiO_2 has 0.04 more vacant d states per Pt atom than bulk Pt, with the number of unfilled d states for Pt/TiO_2 decreasing slightly upon increasing the reduction temperature from 473 to 698°K. In contrast, the number of unfilled d states is significantly higher for Pt/SiO_2, being 0.07 holes per Pt atom greater than for bulk Pt (Table 1).

EXAFS Studies

The EXAFS data taken at liquid nitrogen temperature under static H_2 for the 3.1 and 1.7 wt% Pt/TiO_2 samples after H_2 reduction of the samples at the indicated temperature are shown in Fig. 5. The EXAFS function ($\chi(k)$) is plotted against the photoelectron wave vector (k) after the smooth background decay has been subtracted from the data above the absorption edge. As expected for these highly dispersed systems,

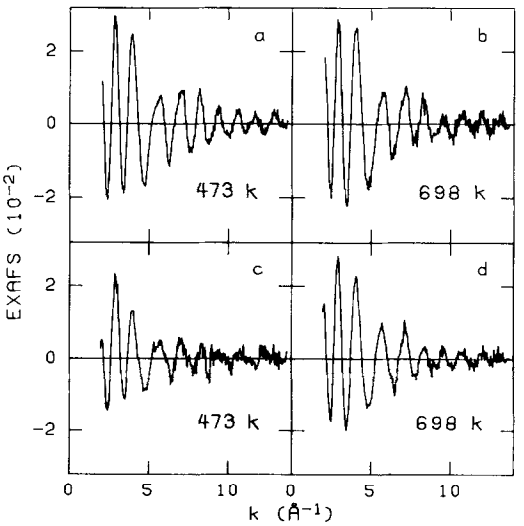

FIG. 5. Normalized EXAFS data of 3.1 wt% Pt/TiO_2 (a and b) and of 1.7 wt% Pt/TiO_2 (c and d) after H_2 reduction at the indicated temperatures.

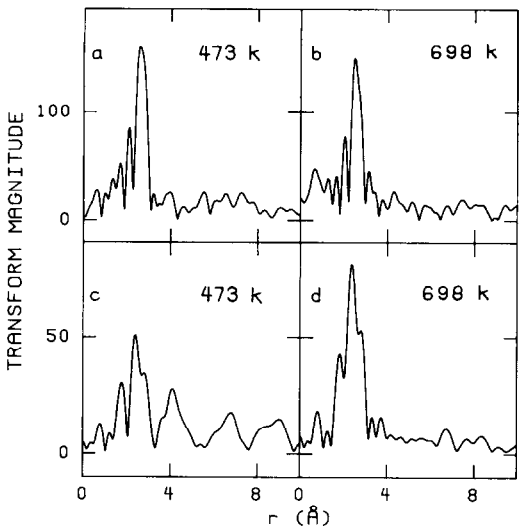

FIG. 6. Fourier transforms of k^3-weighted EXAFS of 3.1 wt% (a and b) and 1.7 wt% (c and d) Pt/TiO_2 after H_2 reduction at the indicated temperatures.

the EXAFS data are much lower in amplitude for all samples than the corresponding data for the 1-μm Pt foil. The foil data are not shown but are in agreement with other published data on Pt foils (*13, 15*). The periods of the EXAFS oscillations and the shapes of the scattering envelopes are very similar for all samples in Fig. 5. This suggests that the first coordination shells of all samples are predominantly Pt and that there is no significant rearrangement of the local Pt environment in going from the low- to the high-temperature H_2 reduction conditions.

Whereas the amplitudes of the EXAFS functions for the 698°K H_2 reduction of the two Pt/TiO_2 samples are roughly similar, indicating that a structurally similar state is being produced by high-temperature H_2 reduction in both cases, the amplitude of the EXAFS data for the 473°K H_2 reduction of the 1.7 wt% Pt/TiO_2 sample is significantly smaller relative to that of all other samples. Thus, there would appear to be a significant change in the highly dispersed 1.7 wt% Pt/TiO_2 catalyst upon increasing H_2 reduction temperature. This change can initially be attributed to an increase in the average first-shell coordination number. This type of change is not observed in the case of the 3.1 wt% Pt/TiO_2.

The Fourier transforms of the k^3-weighted extended fine structure of the two Pt/TiO_2 catalysts after 473 and 698°K H_2 reduction are shown in Fig. 6. The 1.7 wt% data have been transformed over the range from 2.2 to 11.0 $Å^{-1}$ in k-space, and the 3.1 wt% data have been transformed over the range from 2.2 to 13.7 $Å^{-1}$. There is a slight shift in peak position toward shorter R with increasing H_2 reduction temperature; both the peak distance and the shape of the fine structure envelopes in Fig. 5 suggest that the main peak for each curve in Fig. 6 corresponds to a first coordination shell consisting of Pt atoms. Evidence for higher coordination shells is slight since the peak intensities at appropriate distances are on the order of the noise for the 3.1 wt% Pt/TiO_2 (Figs. 6a and b). In the case of the 1.7 wt% Pt/TiO_2, there is no evidence for higher shells (Figs. 6c and d). This confirms that the samples are highly dispersed.

To quantitatively analyze these data, the main peak of each transform was isolated by Fourier filtering below 1.0 Å and above 3.5 Å and was back transformed to k space. The resulting inverse transforms were then analyzed by two procedures. First, coordination numbers and relative disorders for the Pt/TiO_2 were obtained relative to the first shell of bulk Pt using the ratio technique described elsewhere (*29*). The resultant values are listed in Table 2. The data were also analyzed by a four-parameter fitting procedure using the bulk metal first-shell Pt–Pt parameters to obtain the first-shell distance, R_1, the coordination number N_1, and the relative mean square disorder, $\Delta\sigma_1^2$; the resultant values are also given in Table 2. Reference values (Table 2) for the first Pt–Pt shell are from crystallographic data (*30*); the resulting fits are shown in Fig. 7.

These analyses assumed that the inverse data correspond to a coordination shell composed of only one Pt–Pt interaction.

TABLE 2

EXAFS Parameters of Pt/TiO_2

Sample	Reduction temp. (°K)	Reduction time (h)	Ratio technique		Fitting technique		
			N_1	$\Delta\sigma^2 \times 10^3$ (Å^2)	R (Å)	N_1	$\Delta\sigma^2 \times 10^3$ (Å^2)
3.1 wt% Pt/TiO_2	473	1.0	7.2	5.6	2.74	6.0	4.3
3.1 wt% Pt/TiO_2	573	1.5	7.7	9.2	2.70	5.3	5.9
3.1 wt% Pt/TiO_2	698	1.0	7.6	6.4	2.69	5.9	5.0
1.7 wt% Pt/TiO_2	473	2.0	4.5	8.7	2.73	5.0	10.7
1.7 wt% Pt/TiO_2	698	1.0	9.1	10.7	2.69	6.4	7.1
Pt Foil, EXAFS transform	—	—	12	—	2.77	12	1.7
Estimated errors			±2	±1.0	±0.03	±1	±0.5
Bulk Pt, crystallographic			12[a]		2.77[a]	12[a]	

[a] Crystallographic values from Ref. (*23*).

Because of the models proposed by others (*7, 11*), we have also tested the appropriateness of our single shell interaction model with the possibility of multiple shell interactions by fitting the inverse transforms with various combinations of Pt–Pt, Pt–O, and Pt–Ti coordination shells. This was accomplished using fitting programs developed at North Carolina State University and required model data which were obtained from experimental studies of well-characterized materials, such as Pt foils and oxides of platinum for Pt–Pt and Pt–O parameters, and from theoretical parameters published by Teo and Lee (*28*) for Pt–Ti parameters. None of the multiple-shell fits improved on the quality of the single Pt–Pt shell fits with physically reasonable parameters; in fact, all of the multiple shell models gave markedly poorer fits than the fit with the single-shell model. Thus, we can find no evidence for Pt–Ti or Pt–O distances with coordination greater than 1/2 atom/Pt atom, for either low- or high-temperature H_2 reduction of Pt/TiO_2, even though these samples were very highly dispersed as shown by EXAFS and all other characterization techniques.

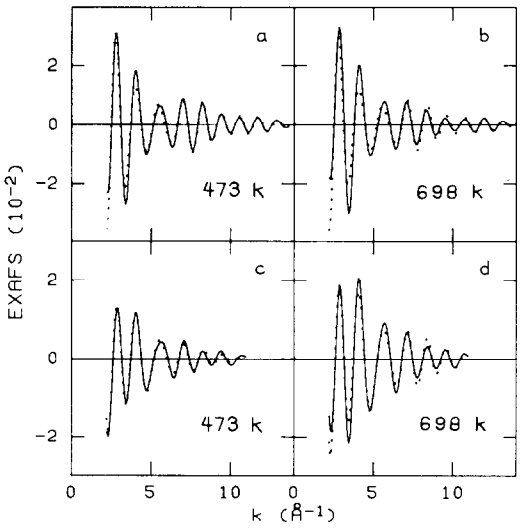

FIG. 7. Inverse transforms (χ_1 vs. k) of the first coordination shell for the experimental data (—) for 3.1 wt% Pt/TiO_2 (a and b) and for 1.7 wt% Pt/TiO_2 (c and d) compared with calculated spectra (---) obtained using parameters from a single Pt–Pt shell fit obtained by minimizing residuals relative to first-shell coordination number, relative disorder, and distance.

DISCUSSION

First, for the Pt/TiO_2 samples the absorption edge studies indicate that there is always a greater number of unfilled d states than for bulk Pt, indicating a transfer of

charge to the TiO_2. Superimposed on this it is observed that an increase in the temperature of H_2 reduction for both the 1.7 and 3.1 wt% Pt/TiO_2 results in a small decrease in the normalized areas in the near-edge region of both the L_{III} and L_{II} absorption edges (Figs. 1 to 4 and Table 1). This suggests a very small but significant increase in the average electron density on the platinum atoms with increasing H_2 reduction temperature; this is clearly shown by the *d*-band vacancy calculations using the combined L_{III} and L_{II} edge areas (Table 1) (*25*). This provides support for the suggestion (*7, 11*) that for higher H_2 reduction temperatures in the Pt/TiO_2 system there is increased electron donation from the support to the Pt atoms. However, it is also quite apparent that the change in average electron donation to Pt with increasing reduction temperature is much smaller than the donation of 0.6 ± 0.1 electron per Pt atom that has been suggested on the basis of theoretical calculations (*7*) or from experiments with single crystals (*9*). We estimate that the change in electron donation is less than 0.02 electrons per Pt atom for our very small crystallites. It would be expected that the electron donation would be highest on a per Pt atom basis for the most highly dispersed Pt; we have achieved very highly dispersed Pt by our "ion-exchange" preparation technique, yet the amount of change in electron transfer with increasing H_2 reduction temperature is very small and no more than for the Pt/TiO_2 prepared by impregnation.

Several other observations may be made from the absorption edge results. The L_{III} edge peak of our 0.7 wt% Pt/SiO_2 is much broader than that of the bulk Pt white-line peak, indicating the existence of unoccupied *d* states extending several electron volts above the threshold edge. The L_{III} edges of the Pt/TiO_2 samples have the same peak height as that of the Pt/SiO_2 sample, but the white-line peaks of the Pt/TiO_2 are markedly narrower on the high-energy side after the 698°K H_2 reduction. Even after H_2 reduction of the Pt/TiO_2 at 473°K, a condition having nothing to do with the so-called SMSI state, the white-line peaks are significantly narrower than for the Pt/SiO_2 which had been treated equally and was about equally dispersed. In the case of the L_{II} absorption edges, the near-edge area of the Pt/TiO_2 is intermediate between the corresponding areas for the Pt/SiO_2 and the bulk Pt. The Pt/TiO_2 has a lower number of unoccupied *d* states than the Pt/SiO_2 reduced and examined under identical conditions (Table 1). Even after H_2 reduction at only 473°K, this effect is relatively pronounced (Table 1), showing very clearly that the support (SiO_2 vs. TiO_2) is having a marked effect on the electron density of the metal. This is occurring under H_2 reduction conditions that give Pt/TiO_2 that adsorbs H_2 and CO normally, i.e., adsorbs H_2 and CO to the same extent that Pt/SiO_2 does. This is not an SMSI state (*3–7*); yet the SiO_2 is influencing the Pt more than is the TiO_2. The change in *d*-electron vacancies for Pt/TiO_2 observed upon H_2 reduction at 698°K as contrasted with 473°K reduction is much smaller than the difference between Pt/TiO_2 and Pt/SiO_2 after H_2 reduction of both at 473°K (Table 1). Therefore the almost total loss of H_2 and CO adsorption capability of Pt/TiO_2 upon high-temperature (698°K) H_2 reduction, the "so-called" SMSI effect, is *not* due to marked changes in the extent of electron transfer from the TiO_2 to the Pt as has been suggested (*7, 9, 11*) but must be due to much more subtle and specific changes in the electronic structure of the Pt atoms which occur upon high-temperature H_2 reduction.

Concern has been expressed that the presence of H_2, presumably chemisorbed on the active metal crystallties during acquisition of data, could mask a significant portion of any electron donation from Ti to Pt atoms. This possibility cannot be dismissed, but we believe it to be unlikely. The magnitude of calculated unfilled *d* states given in Table 1 are in themselves much

less than the suggested value of 0.6 electrons per Pt atom (*7, 9*). Furthermore, we have verified that, after a high-temperature reduction (e.g., at 698°K), there is little or no chemisorption of hydrogen on these Pt/TiO_2 materials. If the degree of increase of electron density on Pt atoms of Pt/TiO_2 with increasing reduction temperature is greater than indicated in Table 1, this would require a significant donation of electron density from H_2 or H atoms after the lower temperature reduction alone. The presence of H_2 during the study of Pt/SiO_2 samples and the apparent decrease in electron density on these materials relative to Pt foil, or relative to 473°K-reduced Pt/TiO_2, refutes this. Alternatively, if the observed decrease in electron density relative to Pt foil is indeed due to electron withdrawal by H_2 and not due to electronic structural changes intrinsic to such small crystallites of Pt, then a concurrent loss of H_2 chemisorption (and electron withdrawal) and electron donation from Ti to Pt atoms after high-temperature reduction should artificially enhance the effect under investigation.

The EXAFS results (Figs. 5 to 7, Table 2) provide further insight into the effect of TiO_2 on Pt. The samples of Pt/TiO_2 prepared by different techniques appear to be similar. Results for both samples are consistent with small, highly dispersed metal particles. The first-shell Pt–Pt distance in both Pt/TiO_2 samples varies between 2.69 and 2.74 Å, dependent upon the H_2 reduction temperature (Table 2). These distances are in all cases smaller than the bulk first-shell Pt–Pt distances of 2.77 Å (*23*) and are smaller than observed for highly dispersed Pt/SiO_2, which is similar to that of the bulk metal and independent of reduction temperature. Furthermore, this interatomic Pt–Pt distance decreases consistently with increasing H_2 reduction temperature (Table 2). The main peak in each case is much reduced in magnitude relative to the peak of the first Pt–Pt coordination shell for bulk Pt analyzed in the same matter, indicating a significantly lower coordination number and/or more disorder in this shell relative to bulk Pt.

There are significant differences between the results of the ratio analysis and the fitting analysis, with the ratio technique generally showing both larger coordination numbers and larger relative disorders. The ratio analysis has larger errors associated with it, since the k^3-weighted transform is more sensitive to the somewhat noisy EXAFS data found at high k. Thus, we feel that the fitting results are more reliable and that the ratio results should be viewed as generally in agreement with them.

The calculated coordination numbers for the 3.1 wt% Pt/TiO_2 reduced in H_2 at 473 and 698°K are the same (Table 2). In contrast, the 1.7 wt% Pt/TiO_2, prepared by ion exchange, has a lower coordination number after 473°K H_2 reduction (Table 2), and it apparently consists of smaller, more highly dispersed clusters of Pt atoms. After H_2 reduction at 698°K this sample of Pt/TiO_2 appears to have a slightly higher first-shell coordination number. We attribute this change to further clustering of the Pt atoms, forming larger clusters from the very small clusters originally formed.

It has been suggested (*7, 11*) that a strong and direct Ti–Pt interaction might account for the unusual H_2 and CO chemisorption results accompanying high-temperature H_2 reduction of Pt/TiO_2 (*3–6*). Therefore, one likely model of the backscattering represented by the main peaks in the transforms of the 698°K-reduced Pt/TiO_2 should involve both a Pt–Pt and Pt–Ti coordination shell about the absorbing Pt atom. Such a model was seriously investigated in our attempt to fit the experimental inverse transforms in Fig. 7, as were other models involving various Pt–O interactions and combinations of shells of different atoms. In all cases and for any combination of Pt–Pt, Pt–Ti, and Pt–O coordination shells, unreasonable parameter values were required to yield good fits with the experimental data; our fitting results are only consistent with a platinum near-neighbor coordination

shell containing significantly less than one Ti or O atom. Conversely, if there exists a strong, direct structural interaction between Pt and Ti atoms or ions or oxygen anions after high-temperature reduction, this interaction must involve not more than 1 out of 10 Pt atoms in small Pt atom clusters on TiO_2. Therefore, there is *no* evidence in these EXAFS data for a strong, extensive, and repetitive Pt–Ti or Pt–O distance or interaction that might provide a structural reason for the observed decrease in H_2 and CO chemisorption after high-temperature H_2 reduction (*3, 4*).

SUMMARY AND CONCLUSIONS

These results clearly rule out most of the possible physical models advanced to date that might explain the marked reduction in CO and H_2 chemisorption. They support the conclusion that the loss in chemisorption is not due to marked sintering or crystallite size growth; dispersion changes very little upon high-temperature reduction as indicated by first-shell coordination number (Table 2) and the evident absence of higher shells in the radial structure function (Fig. 6). Reduction of H_2 and CO chemisorption cannot be due to Pt being buried in or incorporated into the support to a significant extent and cannot be due to reduced Ti covering the Pt clusters or particles; any such model would require a significant Pt–Ti or Pt–O contribution to the backscattering, which was not found. Similarly the results show that there is not epitaxy between the Pt and the surface of the TiO_2; such a situation should also have resulted in a Pt–Ti or Pt–O contribution to the backscattering as well as a lengthening of the Pt–Pt bond. From a structural point of view, the primary, most important, and controlling interactions are the Pt–Pt interactions; Pt-support interactions are clearly only of secondary importance.

The combined x-ray edge and EXAFS results presented here suggest to us that the principle observed effect of the metal-support interaction between TiO_2 and Pt, i.e., the drastic reduction in H_2 and CO chemisorption after reduction at high temperature, is *not* caused primarily by structural changes which necessarily include a close approach of a significant fraction of Pt atoms to the Ti or O ions of the support (*11*). In addition, these results indicate that there is a small but significant electron transfer from the Pt to the TiO_2 after 473°K H_2 reduction, that this transfer is already present almost to its maximum observed extent after 473°K H_2 reduction, a reduction condition that results in no reduced H_2 or CO chemisorption. High-temperature reduction results in a minimal amount of electron transfer from the TiO_2 to the Pt; this amount is less than 0.02 electrons per Pt atom, much less than previously suggested (*7, 11*). The electron transfer that occurs is seen as a loss of *d*-electron vacancies, which are probed by changes in transition probability in the near-edge region between 5 and 20 eV above the edge.

The high-temperature H_2 reduction conditions used here result in marked reductions in H_2 and CO chemisorption, even though the effect of H_2 reduction temperature on charge transfer is very small. Therefore, the effect of the small amount of electron transfer that occurs upon high-temperature reduction is subtle but very pervasive. It may be that certain *d* orbitals are specific for the binding of hydrogen and CO and must have the proper symmetry, direction, and level of electron occupancy. Transfer of a small amount of additional electron charge along with other metal-support interactions (bonding or ligand effects) may cause a rearrangement or rehybridization of the metal–metal bonding which is suggested by the significant decrease in the Pt–Pt distances. This may result in a filling or change in symmetry of the *d* orbitals extending outward from the Pt atoms so that they can no longer contribute to bond formation with hydrogen or

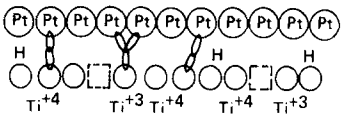

FIG. 8. Schematic model of interactions between small Pt cluster and TiO_2 surface, illustrating the range of metal-support interactions involved; interactions are not limited to a single frequent or periodic bonding.

CO, resulting in a drastic reduction in CO and H_2 chemisorption. Therefore we favor a model for the metal-support interaction such as that shown in Fig. 8. The central features of this model are that the Pt–Pt bonding is of primary importance and that periodically repeated specific metal-support interactions are not required. It is quite likely that direct bonding-type interactions occur between some Pt atoms and certain surface Ti^{3+} ions, and surface oxygen anions, but we infer that one such ligand interaction does not dominate with high frequency or regularity. We infer that the interaction involves a number of different Pt, O, and Ti orbitals across the region where a small Pt cluster is in contact with the TiO_2 surface. This interaction may also be viewed as an interaction of the band structure of the TiO_2 and the developing band structure of the small Pt clusters. The interaction may be sufficiently strong to cause the Pt clusters to take on raft-like configurations rather than the expected three-dimensional particle configuration (*5, 6*), or the raft-like structure may be due to the rehybridization that occurs and thus may be due to bonding factors.

ACKNOWLEDGMENTS

This work was supported in part by the National Science Foundation under Grants DMR 80-11946 (D.E.S.) and CPE 80-20209. Some of the materials incorporated in this work were developed at SSRL with the financial support of the National Science Foundation under Contract DMR 77-27489 in cooperation with the Department of Energy. We gratefully acknowledge the assistance of the SSRL staff and Dr. R. J. Emrich in the acquisition of the data presented here. The Pt/TiO_2 samples were prepared by Dr. Kaiza Saito and Dr. Taka Fukushima, and Dr. Michael Sand prepared the Pt/SiO_2. The TEM characterization was provided by Dr. Michael J. Kelley and Mr. Robert D. Nicholls.

REFERENCES

1. Sleight, A. W., *Science* **208,** 895 (1980).
2. Sinfelt, J. H., *Science* **195,** 641 (1977).
3. Tauster, S. J., Fung, S. C., and Garten, R. L., *J. Amer. Chem. Soc.* **100,** 170 (1978).
4. Tauster, S. J., and Fung, S. C., *J. Catal.* **55,** 29 (1978).
5. Baker, R. T. K., Prestridge, E. B., and Garten, R. L., *J. Catal.* **56,** 390 (1979).
6. Baker, R. T. K., Prestridge, E. B., and Garten, R. L., *J. Catal.* **59,** 293 (1979).
7. Horsley, J. A., *J. Amer. Chem. Soc.* **101,** 2870 (1979).
8. Chung, Y. W., and Weissbard, W. B., *Phys. Rev. B* **20,** 3456 (1979).
9. Bahl, M. K., Tsai, S. C., and Chung, Y. W., *Phys. Rev. B* **21,** 1344 (1980).
10. Tauster, S. J., Fung, S. C., Garten, R. L., Baker, R. T. K., and Horsley, J. A., 1978 American Chemical Society National Meeting, Washington, D.C., September, 1979, Abstr. INOR 1967.
11. Tauster, S. J., Fung, S. C., Baker, R. T. K., and Horsley, J. A., *Science* **211,** 1121 (1981).
12. Sayers, D. E., Stern, E. A., and Lytle, F. W., *Phys. Rev. Lett.* **27,** 1204 (1971).
13. Sinfelt, J. H., Via, G. H., and Lytle, F. W., *J. Chem. Phys.* **68,** 2009 (1978).
14. Lytle, F. W., Wei, P. S. P., Greegor, R. B., Via, G. H., and Sinfelt, J. H., *J. Chem. Phys.* **70,** 4849 (1979).
15. Via, G. H., Sinfelt, J. H., and Lytle, F. W., *J. Chem. Phys.* **71,** 690 (1979).
16. Fukushima, T., Katzer, J. R., Sayers, D. E., and Cook, J., *in* "Proceedings, Seventh International Congress on Catalysis," p. 79. Elsevier, New York, 1981.
17. Lorntson, J. M., Ph.D. dissertation, Univ. of Delaware, Newark, 1980.
18. Mott, N. F., *Proc. Roy Soc. London* **62,** 416 (1949).
19. Cauchois, Y., and Mott, N. F., *Philos. Mag.* **40,** 1260 (1949).
20. Brown, M., Peierls, R. E., and Stern, E. A., *Phys. Rev. B* **15,** 738 (1977).
21. Lewis, P. H., *J. Phys. Chem.* **67,** 2151 (1963).
22. Lewis, P. H., *J. Catal.* **11,** 162 (1968).
23. Lytle, F. W., *J. Catal.* **43,** 376 (1976).
24. Gallezot, P., Weber, R., Dalla Betta, R. A., and Boudart, M., *Z. Naturforsch.* **34a,** 40 (1979).

25. Mansour, A. N., Sayers, D. E., and Cook, J. W., Jr., in preparation.
26. Mansour, A. N., Cook, J. W., Jr., Sayers, D. E., and Katzer, J. R., submitted for publication.
27. Winick, H., and Bienenstock, A., *Amer. Rev. Nucl. Part. Sci.* **28,** 33 (1978).
28. Teo, B. K., and Lee, P. A., *J. Amer. Chem. Soc.* **191,** 2815 (1979).
29. Sayers, D. E., Stern, E. A., and Lytle, F. W., *Phys. Rev. Lett.* **35,** 584 (1975).
30. Pearson, W. B., *in* "A Handbook of Lattice Spacings and Structures of Metals and Alloys," 2nd ed., p. 86. Pergamon, Elmsford, N.Y., 1967.
31. Smith, N. V., Wertheim, G. K., Hufner, S., and Traum, M. M., *Phys. Rev. B* **10,** 3197 (1974).
32. Mattheiss, L. S., and Deitz, R., *Phys. Rev. B* **22,** 1663 (1980).